*https://doi.org/ 10.33472/AFJBS.6.5.2024. 6237-6252*

African Journal of Biological Sciences


# Formulation and evaluation of Ropinirole Nanoparticles loaded nasal *in situ* gels for anti-Parkinson therapy

**CHRISTINA DAS[1*], MURUGANANTHAM V[2], DINTU K P[3]**

[1]Research Scholar, Vinayaka Mission's College of Pharmacy, Salem, Tamil Nadu, India.

[2]Professor, Vinayaka Mission's College of Pharmacy, Salem, Tamil Nadu, India.

[3]Assistant Professor, Department of Botany, Fatima Mata National College (Autonomous), Kollam- 691001, Kerala, India.

**Corresponding author**: Christina Das, Mail id: christe.das@gmail.com

Article History
Volume 6, Issue 5, 2024
Received: 25 May 2024
Accepted: 02 Jun 2024
doi: *10.33472/AFJBS.6.5.2024. 6237-6252*

**Abstract**

Millions of people worldwide are affected by Parkinson's disease (PD), a common neurodegenerative disorder. This research focuses in order to increase the delivery of drugs to the brain and boost therapeutic effects, by the development of ropinirole-loaded chitosan nanoparticle in situ gels for intranasal administration.PD symptoms can be controlled with the help of the dopamine agonist ropinirole. For the Ropinirole loaded chitosan nanoparticles optimization, a Box-Behnken design (BBD) was used. As independent variables, chitosan, sodium tripolyphosphate (TPP), and ropinirole were used. Chitosan nanoparticles that have been loaded with ropinirole were assessed using the following criteria: particle size, PDI, drug entrapment effectiveness, and drug release kinetics. The formation of ropinirole-loaded chitosan nanoparticles with appropriate physicochemical properties was successful, according to the results. The FTIR study confirmed the drug-excipient compatibility. DSC examination revealed information about the thermal behavior of the nanoparticles. The formulated nanoparticles have the potential to improve intranasal delivery of drugs in the treatment of Parkinson's disease. Intranasal administration provides direct access to the central nervous system, avoiding the blood-brain barrier and decreasing systemic adverse effects. The nanoparticles showed prolonged drug release properties which can increase drug concentration in the brain while decreasing dose frequency.

**Keywords:** Ropinirole, chitosan nanoparticle, Parkinson's disease, intranasal drug delivery, Optimization, Formulation development

## Introduction

The most common neurodegenerative movement disorder is Parkinson's disease and it is increasing more rapidly than other neurological disorders worldwide where it is mostly affected in the aging population. Nearly one million individuals globally are living with this disease in the United States [1]

Individuals who are diagnosed with Parkinson's disease usually have gentle growth of nonmotor symptoms for a moderate period of time before the symptoms of movement initiate [2]. The features such as rapid eye movement, disorders in proper sleep, constipation, depression, urinary dysfunction, anosmia are not considered specific symptoms for Parkinson's disease but their occurrence can imply the risk of an eventual Parkinson's diagnosis is high [3]. In advanced countries the calculated prevalence of Parkinson Disease (PD) is around 0.3% in the normal population, 1-3% in the geriatric population; incidence PD rates are approximately in the range of 18 per 100,000 person-years [4].

The consumption of ropinirole orally in solid dosage forms can be challenging due to the factors such as rigidity, twitch, impaired absorption of ropinirole by the patients, gastric dysfunctions etc. For the easiness in administration and quick action of drug there is a high requirement in devise formulations for the delivery of this drug and the challenges can be overcome only through buccal or sublingual delivery of orally dissolving films [5]. Here nasal delivery of ropinirole dug can be chosen for better drug action and it is observed that nasal route exhibits the supremacy of drug delivery to brain when compared with other routes. Since the desired target is brain, this approach is preferable which not only improves the bioavailability by avoiding the first pass metabolism but imparts targeting to the desired site and helps in bypassing the blood brain barrier (BBB). However, it reduces the adverse effects by accomplishing the desired concentration of drug at the site of action and also by supressing any further availability at sites other than targeted area [6].

The nanoparticles can generally be considered to achieve targeted delivery of ropinirole which helps in improving the bioavailability [7]. Apart from this the system can also solubilize drugs for intravascular delivery, in sustaining the effects of ropinirole in tissue and fight against enzymatic degradation such as proteases [8]. The nanoparticles loaded nasal route can be considered for acute or chronic treatments for higher frequency of intake and it results in significant development of drug absorption across the membrane barrier. By undergoing through various techniques such as manipulation of size and unique surface properties, these particles can be refined into smart systems where the nanoparticles can be useful for its ability to preserve drugs from degradation and also deliver it to the targeted site with an adequate controlled release [9].

The use of in situ gels have acquired promising results for controlled release in systemic delivery of drug and local delivery. The in situ gel preparation is able to increase the patient compliance, strengthen the bioavailability of the drug and can be considered as more suitable dosage form for increased action [10]. The administration of in situ gel promotes the formulation to have longer drug release when compared to other system and also helps in sustain release of drug with more effectiveness and higher bioavailability [11] . The other advantage of in situ gel administration is that it’s used to make the drug increase the residence time in the area of use, it thus promotes maximum effectiveness by improving of per cent permeation. Therefore, the delivery of drug via nasal in situ gel is found to be emerging because of its high potential to move or transport the drug to the systemic circulation and to achieve reliability [12].

## 2. Materials

Chitosan, sodium tripolyphosphate (TPP) and ropinirole and were supplied by Loba Chemie, India. All other chemicals were of analytical grade and produced by local vendors.

## 3. Methodology

### Fourier-transform Infrared Spectroscopic analysis:

The compatibility of the drug and excipients were studied by using FTIR Spectroscopy (Alpha II, Bruker, Germany). The sample was prepared by dispersing Ropinirole in KBr in a ratio of 1:3 and compressed to a pellet at a pressure of 600 $kg/cm^2$. The resulting pellet was analysed in spectrophotomer from 4000 $cm^{-1}$ to 400 $cm^{-1}$.

### Differential Scanning Calorimetry

Differential scanning calorimeter (DSC 60, Schimadzu) was employed to get DSC thermograms of pure API or mixtures for determining the Melting Points. Accurately weighed quantity of 1 to 3 mg samples were taken into solid aluminium pans which was sealed and crimped. An empty sealed aluminum pan was kept as a reference. The thermograms were obtained by heating at a rate of 20°C per min with dry nitrogen purging of 20 mL/min.

### S3.1 Experimental Design for synthesis of chitosan nanoparticles

A statistical approach is used to evaluate the importance of the Ropinirole-loaded chitosan nanoparticles formulation using the Box-Behnken design (BBD). For formula optimisation, Stat-Ease; Inc, USA's Design-Expert® programme was employed. Chitosan, TPP, and RPM were chosen as independent variables for Ropinirole-loaded chitosan nanoparticles. Particle size and the Polydispersity index (PDI) were the formulation responses. 15 runs were produced by the program as shown in Table 2 to arrive at the desired formula. Table 1 displays the range of these variables and responses.

*Table 1: Independent variables with their levels and dependent variables with their limitations in the Box Behnken Design for ropinirole-loaded chitosan nanoparticles*

| Name | Goal | Lower Limit | Upper Limit | Lower Weight | Upper Weight | Importance |
|---|---|---|---|---|---|---|
| A: Chitosan | is in range | 0.05 | 0.4 | 1 | 1 | 3 |
| B: TPP (1%) | is in range | 500 | 1500 | 1 | 1 | 3 |
| C: RPM | is in range | 200 | 1200 | 1 | 1 | 3 |
| Particle size | minimize | 100 | 250 | 1 | 1 | 3 |
| PDI | is in range | 0.4 | 0.5 | 1 | 1 | 3 |

### 3.2 Formulation of optimized chitosan Nanoparticles

Chitosan solution was diluted to different concentrations (0.4%, 0.225%, and 0.05%) by adding acetic acid to the stock solution (0.5% w/w) [13]. As per the Box-Behnken design, different volumes of 1% TPP solution were used.

Chitosan nanoparticles were produced by the ionic cross-linking reaction of chitosan with TPP, as described in the literature. Briefly, In ultra-purified water, 20 ml of chitosan solution (0.06mg/ml in 1% acetic acid) and TPP solution (10mg/ml) were made. In addition, 800 uL of 1% TPP was gently added to 20 mL of the previously mentioned chitosan solution with

magnetic stirring at 200 rpm. The interaction of chitosan solution with TPP produced nanoparticles. The resultant nanoparticles were employed in additional research [14].

### 3.3 Formulation of Ropinirole loaded chitosan nanoparticles.

The cross-linking technique was used to formulate ropinirole-loaded chitosan nanoparticles. Approximately 20 ml of chitosan solution (0.06 mg/ml) was blended with 3 ml of ropinirole (2 mg/ml concentration). Another 800 uL of 1% TPP is gently added to the aforesaid drug-polymer combination during magnetic stirring at 200 rpm. lastly, nanoparticles were gathered and employed for additional characterization methods [15].

### 3.4 Evaluation of Ropinirole-loaded chitosan nanoparticles.

#### 3.4.1 Particle Size, Polydispersity Index:

The formulations' PDI and particle size were evaluated using the DLS method (Zeta sizer, Malvern, UK). The formulations' PDI and particle size were assessed using the DLS technique (Zeta sizer, Malvern, UK). Samples were placed into a disposable sized cuvette, filled to a depth of 1 cm, and measurements were made at a temperature of 25 1 °C with light scattering recorded at right angles.

#### 3.4.2. Drug entrapment efficiency

The entrapment efficiency of Ropinirole-loaded Chitosan NP is calculated by ultracentrifugation technique by determining the amount of API that was not entrapped. The EE was calculated by centrifuging formulations at 15000 rpm for 25 min at 4°C. The supernatant was removed, diluted with an appropriate solvent, and then analyzed under UV-Visible spectroscopy at a Lambda max 250nm, in order to determine how much free medicine was present in the formulation [16].

#### 3.4.3. Drug release studies from Chitosan nanoparticles

To a pre-soaked dialysis kit (Pur-A-Lyzer$^{TM}$ Mini Dialysis Kit, Sigma Aldrich) containing 14 KD in 80 ml of simulated nasal fluid (SNF) kept at 37 ±0.5 °C in a 100 ml beaker, 3 ml of Ropinirole loaded chitosan NP dispersion were added.The setup was maintained agitated at 50 rpm on a magnetic stirrer with temperature control. At certain time intervals, 3ml samples were taken and the drug concentration was analyzed using a UV-Visible spectrophotometer (Shimadzu 1800, Japan) at 250nm. sink conditions are maintained with the addition of SNF after every sampling [17].

#### 3.4.4 Drug Release Kinetics

Data on drug release under simulated physiological conditions are necessary for preclinical drug research and will also serve as the basis for regulatory clearances and evaluations of drug products. Using in vitro methods for Nano formulations, it is more common to forecast the in vivo release of the drugs. Mathematical models may be utilized to forecast drug release processes in addition to assisting with formulation development and controlled drug release systems. Complexity occurs in both NP dosage forms and drug release assessment. Therefore, it can be stated that the utilization of in vitro drug release data to predict and characterize drug substances' in vivo performance is a necessary step in the rational development of controlled release formulations [18].

The Drug Release kinetics models include the Korsmeyer-Peppas model, Higuchi Model, First order Release Kinetics Model, and Zero-order Release Kinetics Model.

## 4. Results

### FT-IR spectra

Findings from FT-IR forecast potential interactions between API and formulation excipients. (Figure 1) shows the FTIR spectra of Ropinirole, chitosan, TPP, and ropinirole-chitosan. For ropinirole, the conjugated aldehyde C=O stretch was detected at a wavelength of 1701.88 cm-1, the C-H stretch was detected at wavelengths of 1390.06, 1455.03, and 1759.09 cm-1, and the amine N-H stretch was detected at wavelengths of 2983.53, 2969.45, and 3070.06 cm-1. For Chitosan, alcoholic OH group stretches were detected at 3626.48, 3687.42 and 3733.08 cm-1, Gama-lactam C=O stretch was detected at 1644.47 cm-1, C-H stretch and bending were detected at 892.81, 1373.78 and 1416.50 cm-1, 1° & 2° N-H stretch was noted at 2870.87 and 3283.83 cm-1 & C-O-C bridge stretch was detected at 1149.34 cm-1. In the case of TPP, the corresponding values for P = O stretching, symmetric and antisymmetric stretching vibrations in the PO2 group, symmetric and antisymmetric stretching vibrations in the PO3 group, and antisymmetric stretching of the P-O-P bridge were 1209.50, 1126.72, 1.95.64, and 885.35. Ropinirole-chitosan showed C=O stretching at 1702.17 and 1613.33 cm-1, C-H stretching and bending at 1389.81, 1455.06, 1759.10, 878.84, 1389.81 and 1411.32 cm-1, and amine N-H stretching at 2938.04, 2969.49 and 3070.92 cm-1.

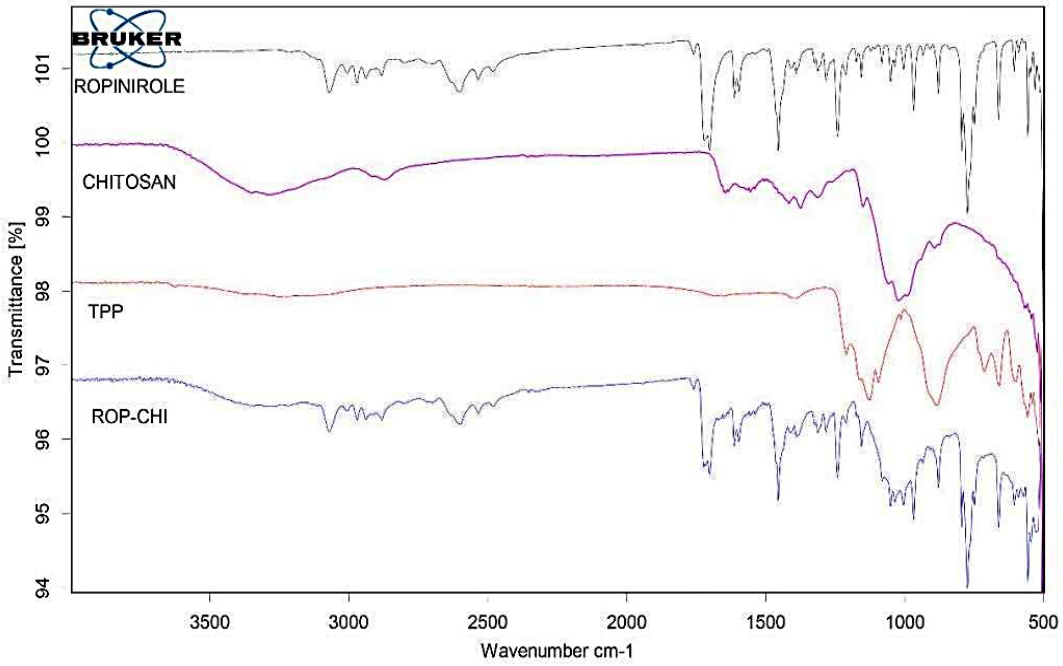


*Figure 1: FTIR spectrum overlay of Ropinirole and excipients*

### Differential Scanning Calorimetry (DSC)

Ropinirole's DSC thermograms revealed a pronounced endothermic peak at 254.22°C (Figure 1s). Chitosan's DSC curve (Figure 2s) revealed endothermic Peak at 128.32°C and exothermic peak at 307.79°C. TPP DSC thermographs revealed endothermic peak at 125.72°C (Figure 3s). Ropinirole-chitosan DSC thermographs demonstrate a peak at 247.06°C in Figure 2.

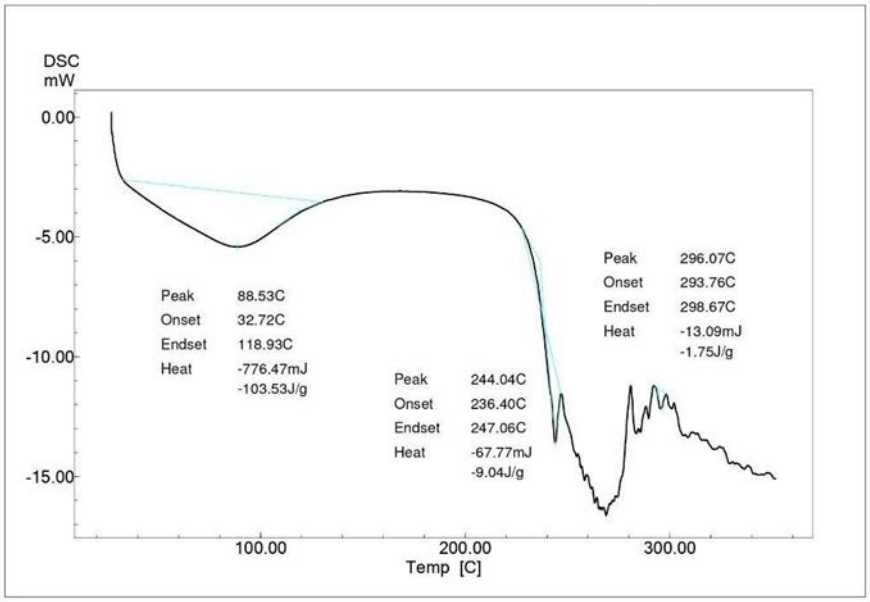


*Figure 2: DSC thermogram of Ropinirole - chitosan*

## Mathematical models for the design of experiments

Three variables (chitosan, TPP, and RPM) were chosen for formulation optimization of ropinirole-loaded chitosan NP by BBD utilizing Design Expert software based on the criteria evaluated during screening trials.

The BBD had suggested 15 trial runs, and the results of trials are shown in Table 2.

*Table 2: BBD Trial runs and observed values of responses for optimization of Ropinirole-loaded chitosan nanoparticles*

| | | Factor 1 | Factor 2 | Factor 3 | Response 1 | Response 2 |
|---|---|---|---|---|---|---|
| **Std** | **Run** | **A: Chitosan** | **B: TPP (1%)** | **C:RPM** | **Particle size** | **PDI** |
| | | **%** | **µL** | | **nm** | |
| 5 | 3 | 0.05 | 1000 | 300 | 120.3 | 0.516 |
| 3 | 11 | 0.05 | 1500 | 900 | 326.6 | 0.595 |
| 1 | 13 | 0.05 | 500 | 900 | 801 | 0.774 |
| 7 | 14 | 0.05 | 1000 | 1500 | 713.3 | 0.756 |
| 12 | 1 | 0.225 | 1500 | 1500 | 768.3 | 0.354 |
| 9 | 5 | 0.225 | 500 | 300 | 432.3 | 0.453 |
| 15 | 6 | 0.225 | 1000 | 900 | 224.9 | 0.414 |
| 13 | 8 | 0.225 | 1000 | 900 | 625.1 | 0.36 |
| 10 | 10 | 0.225 | 1500 | 300 | 407.2 | 0.398 |
| 14 | 12 | 0.225 | 1000 | 900 | 410.9 | 0.424 |
| 11 | 15 | 0.225 | 500 | 1500 | 355.2 | 0.456 |
| 2 | 2 | 0.4 | 500 | 900 | 1503 | 0.441 |
| 4 | 4 | 0.4 | 1500 | 900 | 812.5 | 0.58 |
| 6 | 7 | 0.4 | 1000 | 300 | 1467 | 0.526 |
| 8 | 9 | 0.4 | 1000 | 1500 | 955.2 | 0.491 |

Depending on the p value, the ANOVA findings identify significant variables. Since they had p values less than 0.05, the parameters chitosan, TPP, and RPM were deemed significant (Table 3).

### 4.2. ANOVA for Linear model

**Analysis of Response 1: Particle size**

*Table 3: ANOVA results for particle size by Box- Behnken Design*

| Source | Sum of Squares | df | Mean Square | F-value | p-value | |
|---|---|---|---|---|---|---|
| **Model** | 1.056E+06 | 3 | 3.519E+05 | 2.94 | 0.0802 | not significant |
| **A-Chitosan** | 9.636E+05 | 1 | 9.636E+05 | 8.06 | 0.0161 | |
| **B-TPP (1%)** | 75446.70 | 1 | 75446.70 | 0.6313 | 0.4437 | |
| **C-RPM** | 16671.38 | 1 | 16671.38 | 0.1395 | 0.7159 | |
| **Residual** | 1.315E+06 | 11 | 1.195E+05 | | | |
| **Lack of Fit** | 1.234E+06 | 9 | 1.372E+05 | 3.42 | 0.2467 | not significant |
| **Pure Error** | 80212.56 | 2 | 40106.28 | | | |
| **Cor Total** | 2.370E+06 | 14 | | | | |

The factor coding is '**Coded**'.

**Type III - Partial** is the sum of squares.

Model significance is shown by the **Model F-value** of 2.94. There is only an 8.02% chance that an F-value this big may arise owing to noise.

**P-values** under 0.0500 suggested that the model terms are important. A is a crucial model term in this scenario. If the value is higher than 0.1000, the model terms are not considered relevant. Model reduction may enhance the model if it has a large number of unimportant model terms (excluding those necessary to enable hierarchy).

The **F-value for the lack of fit**, 3.42, indicates that the lack of fit is not significant in comparison to the pure error. A significant Lack of Fit F-value has a 24.67% possibility of being caused by noise. Given that we want the model to fit, a non-significant lack of fit is desirable.

Following is the final linear equation in terms of the coded factors:

***Particle size = 661.52 +347.06A -97.11B +45.65C***

It is possible to anticipate the reaction for certain amounts of each element using the equation expressed in terms of coded factors. By default, the factors' high values are written as +1 and their low levels as -1. By contrasting the factor coefficients, the coded equation may be used to determine the relative importance of the elements. Here Figure 3 shows the graphical representation of the effect of factors on particle size

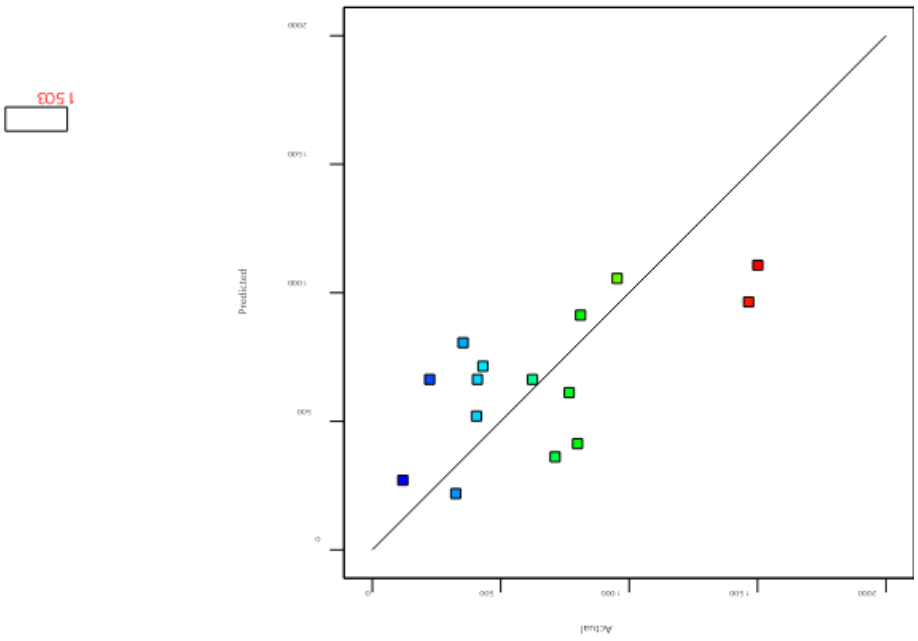

*Figure 3: 3D surface plot demonstrating the effect of factors on the particle size*

## Analysis of Response 2: PDI

*Table 4: ANOVA results for PDI by Box- Behnken*

| Source | Sum of Squares | df | Mean Square | F-value | p-value | |
|---|---|---|---|---|---|---|
| **Model** | 0.2163 | 9 | 0.0240 | 9.44 | 0.0118 | significant |
| A-Chitosan | 0.0455 | 1 | 0.0455 | 17.86 | 0.0083 | |
| B-TPP (1%) | 0.0049 | 1 | 0.0049 | 1.91 | 0.2260 | |
| C-RPM | 0.0034 | 1 | 0.0034 | 1.32 | 0.3024 | |
| AB | 0.0253 | 1 | 0.0253 | 9.93 | 0.0253 | |
| AC | 0.0189 | 1 | 0.0189 | 7.43 | 0.0415 | |
| BC | 0.0006 | 1 | 0.0006 | 0.2170 | 0.6610 | |
| $A^2$ | 0.1164 | 1 | 0.1164 | 45.74 | 0.0011 | |
| $B^2$ | 0.0016 | 1 | 0.0016 | 0.6146 | 0.4686 | |
| $C^2$ | 0.0001 | 1 | 0.0001 | 0.0316 | 0.8659 | |
| **Residual** | 0.0127 | 5 | 0.0025 | | | |
| Lack of Fit | 0.0104 | 3 | 0.0035 | 2.91 | 0.2660 | not significant |
| Pure Error | 0.0024 | 2 | 0.0012 | | | |
| **Cor Total** | 0.2291 | 14 | | | | |

Factor coding is **Coded**.
Sum of squares is **Type III - Partial**

The model is suggested to be significant by the model's F-value of 9.44. The likelihood that noise would result in an F-value this big is merely 1.18%.

Model terms are considered significant when the P-value is less than 0.0500. A, AB, AC and $A^2$ are important model variables in this instance. Model terms are not significant if the value

is higher than 0.1000. Model reduction may enhance your model if there are several unimportant model terms (except those needed to maintain hierarchy).

The F-value for the lack of fit, 2.91, indicates that the lack of fit is not significant in comparison to the pure error. A significant Lack of Fit F-value has a 26.60% likelihood of being caused by noise.

Given that we want the model to fit, a non-significant lack of fit is desirable.

Final linear equation with coding factors:

**PDI = 0.3993 -0.0754A -0.0246B +0.0205C +0.0795AB -0.0688AC -0.0118BC +0.1776A² +0.0206B² -0.0047C²**

For given levels of each factor, the equation in terms of coded factors can be used to make predictions about the response. By default, the factors' high levels are coded as +1 and their low levels as -1. The coded equation can be used to compare the factor coefficients and determine the relative importance of the components. Figure 4 shows 3D graph relationship between various factors on PDI

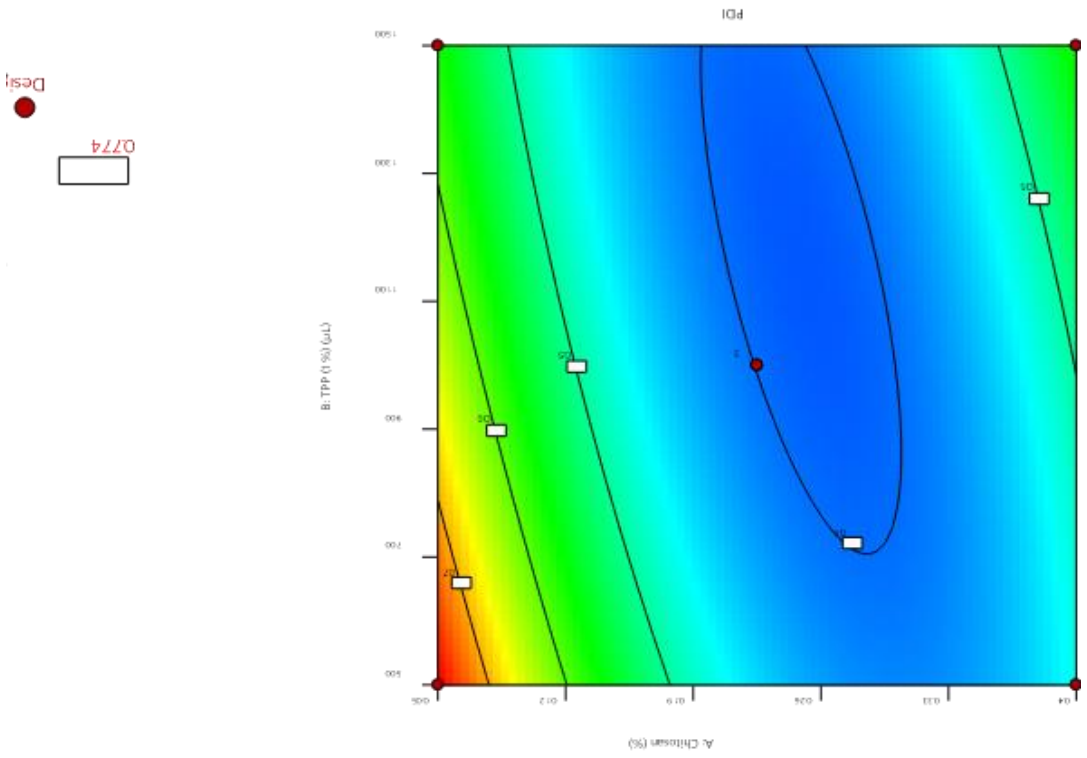


*Figure 4: 3D graphs for demonstrating the relationship between various factors on PDI*

**Number of solutions found through the Design of Experiment (DoE)**

Chitosan, TPP, and RPM were used as the three components in the Design of Experiment (DoE), which produced 68 options from which the one with the highest desirability was selected. The solution is provided in Table 5.

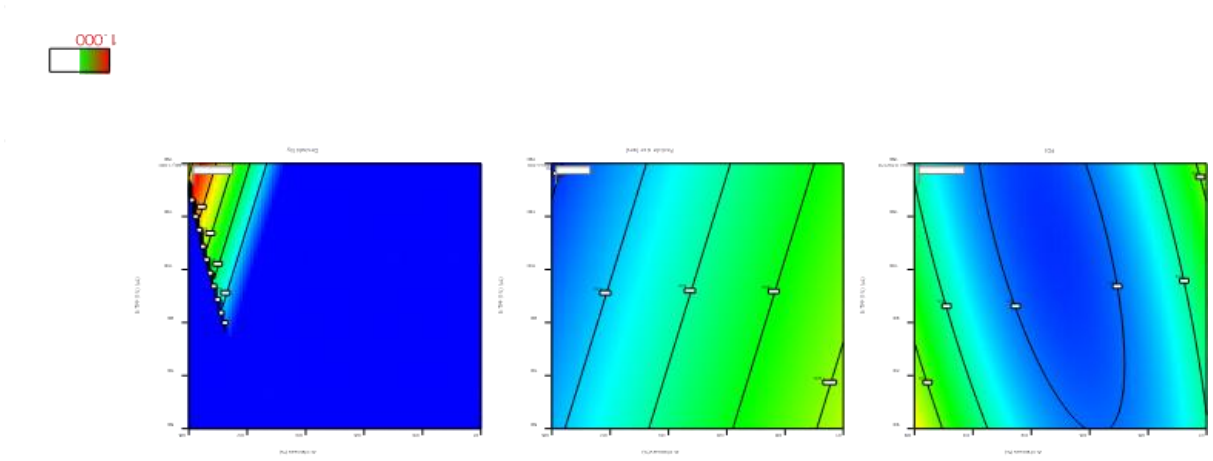

*Figure 5: Demonstrating relationship between factor A and B on desirability, particle size and PDI of all responses*

*Table 5: Predicted vs obtained mean of particle size and PDI*

| Solution 1 of 87 Response | Predicted Mean | Predicted Median | Observed | Std Dev | SE Mean | 95% CI low for Mean | 95% CI high for Mean | 95% TI low for 99% Pop | 95% TI high for 99% Pop |
|---|---|---|---|---|---|---|---|---|---|
| **Particle size** | 200 | 200 | | 345.707 | 213.836 | -270.65 | 670.65 | -1564.84 | 1964.84 |
| **PDI** | 0.492178 | 0.492178 | | 0.0504528 | 0.0506509 | 0.361976 | 0.62238 | 0.118293 | 0.866063 |

## Evaluation of Ropinirole-loaded Chitosan Nanoparticles

### Evaluation of particle size, PDI & zeta-potential

The average particle size and PDI of bare chitosan nanoparticles were 139.4 nm and 0.328, respectively. The bare chitosan nanoparticle was discovered to have a zeta potential of 20.0 mV.

Chitosan nanoparticles loaded with ropinirole had an average particle size and PDI of 156.7 nm and 0.241, respectively. Ropinirole-loaded chitosan nanoparticles had a zeta potential of 11 mV.

### Drug entrapment efficiency

Ropinirole-loaded Chitosan NP formulation showed a 91% drug entrapment efficiency.

### Drug Release Kinetics

Different invitro kinetics models were run, and based on the R2 value, it was determined that the first-order model, shown in Table 6, best fit the invitro data. Figure 6 illustrates the drug release pattern from the Ropinirole-loaded chitosan nanoparticles.

*Table 6: Drug release kinetic modelling data of drug release*

| Plot | Slope | R2 value | n | Drug release Mechanism |
|---|---|---|---|---|
| **0 order** | 6.8255 | 0.9159 | | |
| **1st order** | -0.0681 | **0.9917** | | First order drug release |
| **Higuchi** | 0.0347 | **0.9818** | | Fickian Diffusion controlled Drug release |

| | | | | |
|---|---|---|---|---|
| **Kosmeyerpeppas** | 1.2505 | 0.9584 | 1.1281 | |

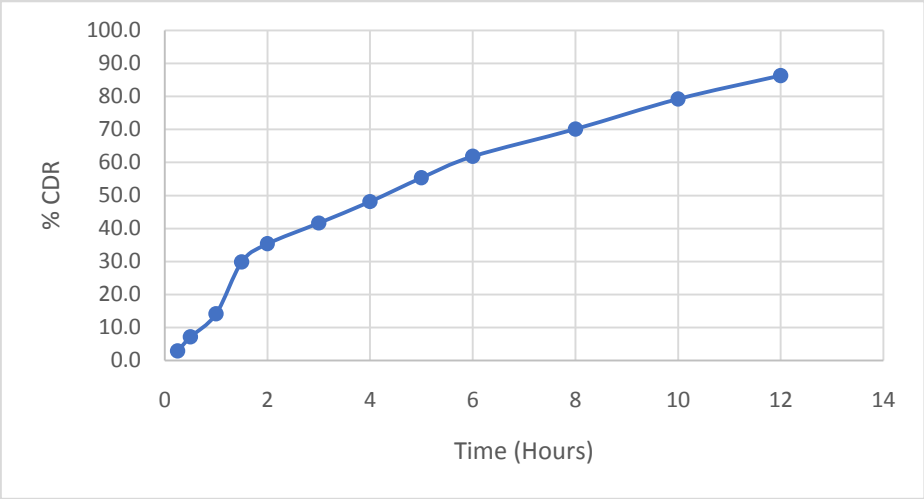


*Figure 6: Release of Ropinirole from chitosan nanoparticles in Physiological pH*

## 5. Discussion

### 5.1. Characterization of Ropinirole-loaded Chitosan Nanoparticles

#### 5.1.1. FT- IR spectra

The FTIR measurements demonstrate that there is no chemical bond between the ropinirole and the preparation's polymer. Therefore, the API and polymer are compatible.

#### 5.1.2. Differential Scanning Calorimetry (DSC)

A decrease in the drug's melting point was seen in the DSC thermogram of the optimised formulation of ropinirole and ropinirole-loaded chitosan nanoparticle, which may be related to a decrease in the compound's crystalline nature.

### 5.2 Formulation studies

#### 5.2.1. Mathematical models for the designing of experiments

Design Expert software was used to demonstrate the response surface methodology (RSM) by integrating the variables. The Box Behnken Design (BBD), a sort of second-order design, is founded on incomplete factorial designs with 3 levels. A Box Behnken (three components at three distinct levels) experimental design was suggested for the optimization of the synthesized NP. A three-part design with two completely leveled factors in each component and one factor set to zero level. Design Expert ® (13.0.5, Stat-Ease Inc., Minneapolis, MN, USA) was used to analyze the quadratic response surfaces and study the second-order polynomial model. BBD can do optimization utilizing fewer experimental trial runs.

#### 5.2.1.1. ANOVA for Ropinirole loaded Chitosan Nanoparticles

**Particle size**

The significance of the model is shown in Table 3 by the F value of 416.03 and the p-value of 0.0002. The result section includes the final regression equation, which takes into account the

values of each coefficient. The effects of each individual variable and their interactions on particle size are shown in the table 3.

**PDI**

The significance of the model is shown in Table 4 by the F value of 9.37 and the p-value of 0.0459. The result section includes the final regression equation, which takes into account the values of each coefficient. The results of the various factors on the PDI are shown in table 4, along with their interactions.

**Using 3D graphs, we can show how different parameters A, B, and C affect the particle size and PDI of the formulation of ropinirole-loaded chitosan nanoparticles.**

Figures 3 and 4 of 3D graphs provide a 3D picture of how each element affects the responses.

### 5.3. Evaluation of Chitosan Nanoparticles

#### 5.3.1. Particle size and PDI

Because the particle size of the optimised formulation is in the nano size range, it can pass through the BBB and the mucus layer to reach the target location.

#### 5.3.2 Zeta potential

Zeta potential is determined to be -23.0 mV and -27.6 mV for the final optimised formulations of chitosan NP and ropinirole-loaded chitosan nanoparticles. Ideal zeta potential is ±30 mV. It suggests that the preparation is stable.

The negatively charged mucus membrane may repel the ropinirole-loaded chitosan nanoparticle if it has a negative zeta potential. This repellency may restrict the nanoparticles' adherence and contact with the mucosal surface, which might have an impact on their penetration and bioavailability. Chitosan itself is known to have mucoadhesive properties, which can help promote interaction with the mucus membrane and improve drug absorption. However, by looking at the other factors, such as the composition, surface modification of the nanoparticles, and also size less than 200nm, can also influence their behavior in nasal delivery [19].

**Drug Release Kinetics:**

Higuchi's mode describes the release of API from an insoluble matrix as the square root of a time-dependent process based on Fickian diffusion [20,21]. The model that best matches the release data was chosen based on the values of the various models' correlation coefficients. The Higuchi model's higher R2 values (0.98) provided evidence for the hypothesis that drug release from Chitosan NPs was diffusion-controlled [15].

**Conclusion**

A possible strategy for improving drug delivery to the brain is the formulation of ropinirole-loaded chitosan nanoparticles for intranasal administration in Parkinson's disease utilising the Box-Behnken design. The intranasal route has various benefits, including needle-free administration, non-invasiveness, and direct delivery to the central nervous system (CNS). Parkinson's disease is a common neurodegenerative condition. Overall, the formulation of ropinirole-loaded chitosan NP for intranasal administration shows promise in terms of enhancing the targeted transport of API to the brain for the treatment of Parkinson's disease.

Bypassing the blood-brain barrier, increasing drug concentration in the brain, and lowering dosage frequency while reducing systemic adverse effects are possible with this strategy.

**Conflict of Interest:** The author declares no conflict of interest.

**Acknowledgement**
We would like to express my sincere gratitude to Vinayaka Mission's College of Pharmacy, Salem, Tamil Nadu, India, for providing the necessary facilities and support for conducting this research as part of my PhD work. The conducive academic environment and resources offered by the institution have been instrumental in the successful completion of this project.

Furthermore, we extend our heartfelt appreciation to Nazareth College of Pharmacy, Othera, Thiruvalla, Kerala, India, and Fatima Mata National College (Autonomous), Kollam-691001, Kerala, India, for their invaluable contributions to this work. Their collaboration and assistance have enriched the research process and enhanced the quality of outcomes.

**References**

[1] Armstrong MJ, Okun MS. Diagnosis and Treatment of Parkinson Disease: A Review. JAMA - Journal of the American Medical Association 2020;323:548–60. https://doi.org/10.1001/jama.2019.22360.

[2] V AN, George P, L DA. Application of 32 Factorial D-Optimal Design in Formulation of Porous Osmotic Pump Tablets of Ropinirole; An Anti-Parkinson's Agent. Journal of Young Pharmacists 2017;9:87–93. https://doi.org/10.5530/jyp.2017.9.17.

[3] Berg D, Postuma RB, Adler CH, Bloem BR, Chan P, Dubois B, et al. MDS research criteria for prodromal Parkinson's disease. Movement Disorders 2015;30:1600–11. https://doi.org/10.1002/mds.26431.

[4] Balestrino R, Schapira AHV. Parkinson disease. Eur J Neurol 2020;27:27–42. https://doi.org/10.1111/ene.14108.

[5] Lai KL, Fang Y, Han H, Li Q, Zhang S, Li HY, et al. Orally-dissolving film for sublingual and buccal delivery of ropinirole. Colloids Surf B Biointerfaces2018;163:9–18. https://doi.org/10.1016/j.colsurfb.2017.12.015.

[6] Jafarieh O, Md S, Ali M, Baboota S, Sahni JK, Kumari B, et al. Design, characterization, and evaluation of intranasal delivery of ropinirole-loaded mucoadhesive nanoparticles for brain targeting. Drug Dev Ind Pharm 2015;41:1674–81. https://doi.org/10.3109/03639045.2014.991400.

[7] Bhattamisra SK, Shak AT, Xi LW, Safian NH, Choudhury H, Lim WM, et al. Nose to brain delivery of rotigotine loaded chitosan nanoparticles in human SH-SY5Y neuroblastoma cells and animal model of Parkinson's disease. Int J Pharm 2020;579:119148. https://doi.org/10.1016/j.ijpharm.2020.119148.

[8] Bikiaris D, Karavelidis, Karavas, Giliopoulos, Papadimitriou. Evaluating the effects of crystallinity in new biocompatible polyester nanocarriers on drug release behavior. Int J Nanomedicine 2011:3021. https://doi.org/10.2147/ijn.s26016.

[9] Luppi B, Bigucci F, Cerchiara T, Zecchi V. Chitosan-based hydrogels for nasal drug delivery: From inserts to nanoparticles. Expert Opin Drug Deliv 2010;7:811–28. https://doi.org/10.1517/17425247.2010.495981.

[10] Rao M, Agrawal DK, Shirsath C. Thermoreversible mucoadhesive in situ nasal gel for treatment of Parkinson's disease. Drug Dev Ind Pharm 2017;43:142–50. https://doi.org/10.1080/03639045.2016.1225754.

[11] Basu A, Masareddy RS, Patil A, Bolmal U. Design and characterization of sustained release in situ gastric floating gel of ropinirole hydrochloride. Indian Journal of Pharmaceutical Education and Research 2021;55:374–82. https://doi.org/10.5530/ijper.55.2.75.

[12] Iyan Sopyan, Wulan Intani, Insan Sunan K S, Cikra Ikhda N H S. The Advantages of In situ Gel from Every Different Formulation. International Journal of Research in Pharmaceutical Sciences 2020;11:7198–206. https://doi.org/10.26452/ijrps.v11i4.3845.

[13] Tanasale MFJDP, Bijang CM, Rumpakwara E. Preparation of Chitosan with Various Molecular Weight and Its Effect on Depolymerization of Chitosan with Hydrogen Peroxide using Conventional Technique. Int J Chemtech Res 2019;12:112–20. https://doi.org/10.20902/IJCTR.2019.120113.

[14] Balde A, Hasan A, Joshi I, Nazeer RA. Preparation and optimization of chitosan nanoparticles from discarded squilla ( *Carinosquillamulticarinata* ) shells for the delivery of anti-inflammatory drug: Diclofenac. J Air Waste Manage Assoc 2020;70:1227–35. https://doi.org/10.1080/10962247.2020.1727588.

[15] Jafarieh O, Md S, Ali M, Baboota S, Sahni JK, Kumari B, et al. Design, characterization, and evaluation of intranasal delivery of ropinirole-loaded mucoadhesive nanoparticles for brain targeting. Drug Dev Ind Pharm 2015;41:1674–81. https://doi.org/10.3109/03639045.2014.991400.

[16] Rinaldi F, Hanieh P, Chan L, Angeloni L, Passeri D, Rossi M, et al. Chitosan Glutamate-Coated Niosomes: A Proposal for Nose-to-Brain Delivery. Pharmaceutics 2018;10:38. https://doi.org/10.3390/pharmaceutics10020038.

[17] Galgatte UC, Kumbhar AB, Chaudhari PD. Development of *in situ* gel for nasal delivery: design, optimization, *in vitro* and *in vivo* evaluation. Drug Deliv 2014;21:62–73. https://doi.org/10.3109/10717544.2013.849778.

[18] Herdiana Y, Wathoni N, Shamsuddin S, Muchtaridi M. Drug release study of the chitosan-based nanoparticles. Heliyon 2022;8:e08674. https://doi.org/10.1016/j.heliyon.2021.e08674.

[19] Mikušová V, Mikuš P. Advances in Chitosan-Based Nanoparticles for Drug Delivery. Int J Mol Sci 2021;22:9652. https://doi.org/10.3390/ijms22179652.

[20] Paul DR. Elaborations on the Higuchi model for drug delivery. Int J Pharm 2011;418:13–7. https://doi.org/10.1016/j.ijpharm.2010.10.037.

[21] Bayer IS. Controlled Drug Release from Nanoengineered Polysaccharides. Pharmaceutics 2023;15:1364. https://doi.org/10.3390/pharmaceutics15051364.

# Supplementary data

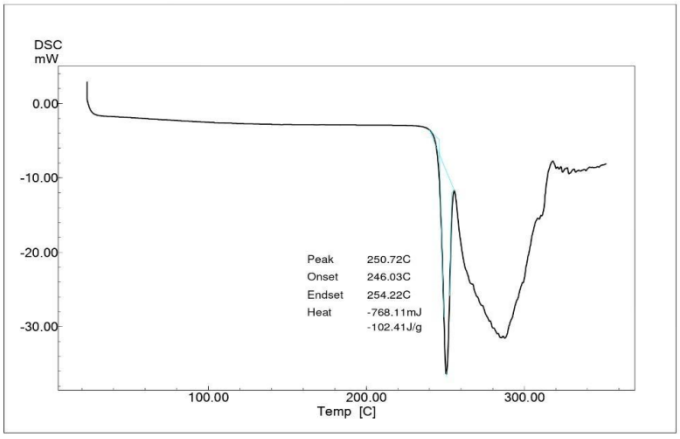


*Figure. 1s: DSC thermogram of Ropinirole*

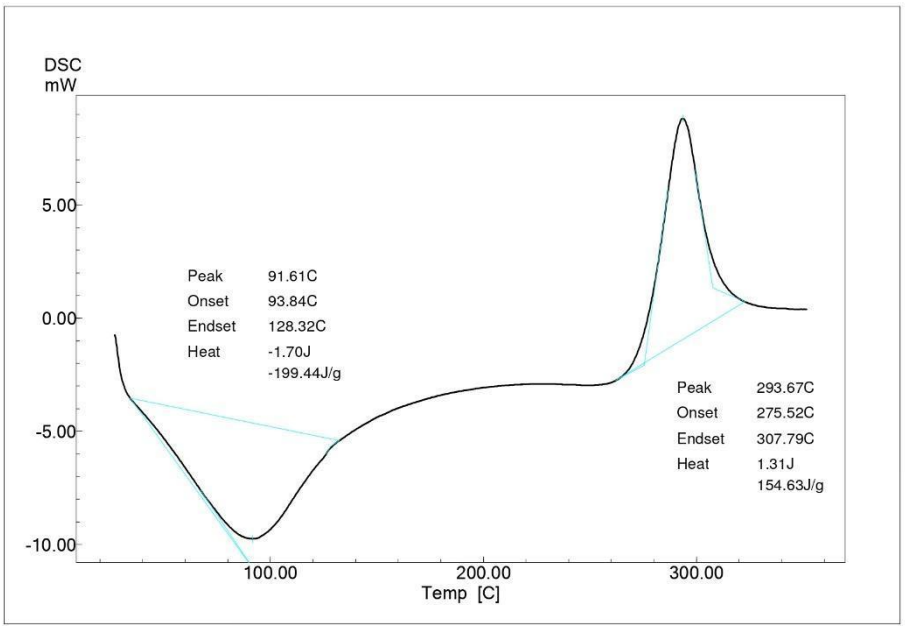


*Figure. 2s: DSC thermogram of Chitosan*

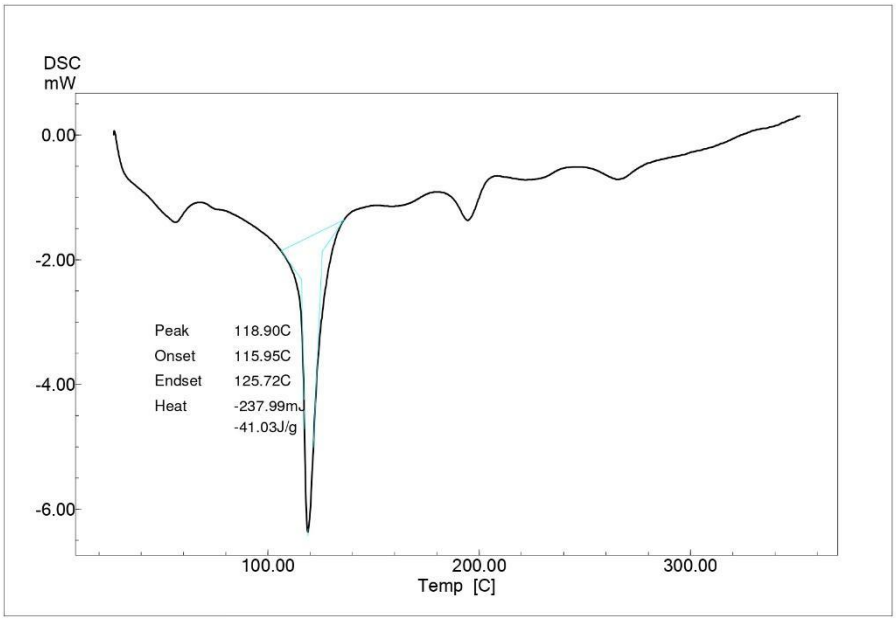


*Figure. 3s: DSC thermogram of TPP*